# Chapter 2

# Theoretical aspects of optoelectronic properties of NPs.

**Abstract**

This chapter represents a concise report of the basic theoretical background regarding the development of the concept of Surface Plasmon (SP) and quantification of the Surface Plasmon Polaritons (SPPs). In the next section different phenomena associated with optical properties of NPs such as Plasmon modes on metal-dielectric interface, excitation of surface Plasmon, light absorption and scattering have been described briefly. The classical and quantum mechanical approaches have been stated and compared to explore the significance of these approaches suited for NPs with different sizes. Several elecrodynamic methods under classical approach have been provided here. Besides these the numerical methods have been mentioned. Among the numerical methods the Discrete Dipole Approximation has been focused specially for its utility in the execution of computational modelling. In case of Quantum mechanical approach, the TDDFT method with its significance in the assessment of optical property of NPs has been stated clearly. The linear response formalism has been presented elaborately due to its inclusion in TDDFT for development of computational modelling.

## 2.1 Theoretical developments of surface plasmons:

The study of plasmons on nanostructures has developed a research field of its own called "plasmonics". There has been a great interest in interpreting the interactions between light and nanoparticles since Michael Faraday's exploration of the optical property of colloidal gold in the mid 1800s.[1] Around fifty years later, the pertinent scientific investigations had been carried ahead by Arnold Sommerfeld[2] in 1899 through theoretical studies and by Robert Wood in 1902,[3] through experimental observations of plasmonic effects in light spectra. However, the theoretical foundation of optical property of NPs was laid in 1908 by Garnett, Mie and Beirträge, explaining the complete theory of electromagnetic radiation of scattering and absorption.[4,5] More comprehensive understanding of surface plasmons was established while a number of theoretical studies had appeared in the 1950s. The early development of plasmonics was inaugurated by the work of Pines, describing the collective oscillation of free electrons as 'plasmon' in 1956.[6] Yet again, the real boom of the research in this field came at the following years of 1960s. The first experimental benchmark of optical excitation of surface plasmons on metal films was explored by Otto,[7] Kretschmann and Raether.[8] in 1968. Kreibic and Zacharias enlightened the optical properties of metal NPs in terms of surface plasmons in 1970.[9] The introduction of the term 'Surface Plasmon Polaritons' was also propped up by Cunningham *et al.* in 1974.[10] In the late 1970s, the technological concern of plasmons started with the discovery of extraordinary enhancements in the Raman Scattering of light by molecules attached to Ag NP, through the investigation of Fleischmann,[11] Duyne and Jeanmarie.[12] In recent times, the follow up works have been extended to several cutting edge developments including the advanced nano fabrication techniques, the expansion of high sensitivity optical characterization schemes and emergence of different numerical simulation algorithms together with the improvement of the computational executions

## 2.2 Excitation of surface plasmon:

The surface plasmon dispersion has been found below the photon dispersion for all energies. The momentum of incident light is found always lower than the momentum of surface plasmon modes. So the surface plasmons cannot be excited by plane wave incident on the interface from the dielectricum. In order to excite surface plasmons, additional momentum has to

be provided. This can be done either by placing a regular grating structure at the interface or by letting the excitation light pass through a medium with a high refractive index (e.g. prism). For the latter case the excitation light can either come from the dielectricum (Otto configuration, 1968) or from the metal side (Kretschmann configuration, 1972). In Otto configuration, the total reflection at the prism/air interface generates an evanescent field that excites the surface plasmons at the dielectric/metal interface. [Figure 2.1 (a)] This method has a limitation of keeping constant distance between the metal and the prism. In Kretschmann configuration, the total reflection at the prism/metal interface generates an evanescent field that excites the surface plasmons at the opposite metal/air interface. [Figure2.1 (b)] In this method the metal film has to be very thin in order to allow the light field to reach through the film.

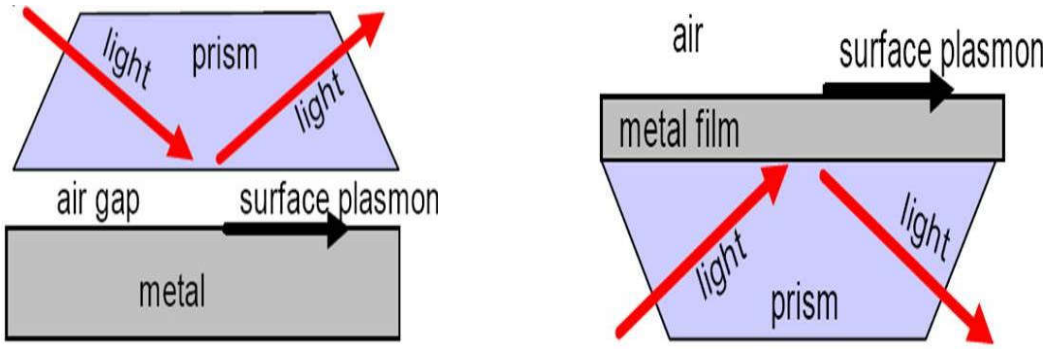


**(a)** **(b)**

**Figure 2.1** **(a)** Otto configuration **(b)** Kretschmann configuration.

## 2.3 Light scattering and absorption by nanoparticles:

At the plasmon resonance frequency, NPs strongly absorb and scatter light. This provides to the brilliant colour display by NPs. The ratio of scattering to absorption changes dramatically with size and shape as shown in the following Figure 2.2. The optical property of large particles (dimension above 30 nm) is dominated by scattering while absorption is dominated in case of small particles.

**Figure 2.2** Nanoparticles of various shape and size in solution – the plasmonic resonance determines the colour.

The light scattering, absorption and extinction particles are described by frequency dependent cross-sections such as $C_{sca}$, $C_{abs}$ and $C_{ext}$, where $C_{ext} = C_{sca} + C_{abs}$. When a particle is illuminated with the light intensity per area $I_0(\omega)/A$, the amount of scattered light is given by:

$$I_{sca}(\omega) = \frac{I_0(\omega)}{A} . C_{sca}(\omega) \tag{2.1}$$

When the cross sections are normalized to particle's geometrical cross sections, new terms called efficiencies such as $Q_{sca}$, $Q_{abs}$ and $Q_{ext}$ are formed.

## 2.4 Derivation of surface plasmon polaritons:

One of the simple models to describe the response of a metallic particle exposed to an electromagnetic field was proposed by Paul Drude.[13,14] According to Drude model, the free electron gas moves freely in between independent collisions such as lattice ions, other electrons, defects, phonons etc. These collisions occur with an average rate of $\gamma_0 = \tau^{-1}$ with $\tau$ being the so called electron relaxation time.

In presence of an external field, the electrons acquire drift motion due to the acceleration resulting from collisions. Only the electrons near the Fermi level contribute, because the Pauli Exclusion Principle does not allow deeper lying electrons to change their electronic state. Band-structure corrections lead to a modification of this motion. These corrections are customarily

incorporated into an effective mass $m^*$, which is in general different from the free-electron mass $m_e$.

Most of the properties of real metals, including their optical properties, are described by the frequency dependent dielectric function $\varepsilon(\omega)$. Here is the frequency of the applied field. This frequency dependent dielectric function can be well predicted from this simple model. The resulting equation is:

$$\varepsilon(\omega) = \varepsilon_\infty - \frac{\omega_p^2}{\omega(\omega + i\gamma_0)} \approx \varepsilon - \frac{\omega_p^2}{\omega^2} + i\frac{\gamma_0\,\omega_p^2}{\omega^3} \tag{2.2}$$

Here $\omega_p$ is the plasma frequency and $\gamma_0$ is the electron relaxation rate. $\varepsilon_\infty$ is the bound electron contribution to the polarizability and should have the value of 1 if only the conduction band electrons contribute to the dielectric function.

The plasma frequency is given by $\omega_p = \sqrt{ne^2/\varepsilon_0\, m^*}$ with $n$ and $m^*$ being the density and effective mass of the conduction electrons, respectively. If $\gamma_0$ and $\varepsilon_\infty$ are neglected for a while, the Drude dielectric function simplifies to $\varepsilon_d = 1 - \omega_p{}^2/\omega^2$ and forms two distinguished frequency regions. When $\omega$ is larger than $\omega_p$, $\varepsilon_d$ becomes positive and the corresponding refractive index $n$ is a real quantity.[15] On the contrary, if $\omega$ is smaller than $\omega_p$, $\varepsilon_d$ becomes negative and $n$ is imaginary.

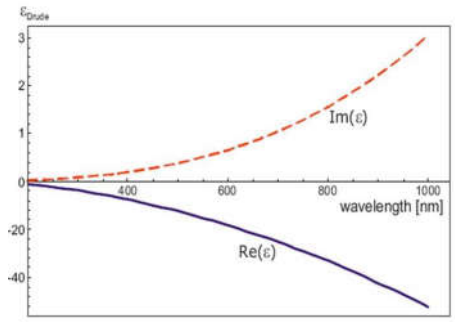


**Figure 2.3** Real and imaginary part of dielectric constant for gold according to the Drude-Sommerfeld free electron model. The blue line is the real part, and the red dashed line is the imaginary part.[16]

The consequence of $\omega < \omega_p$ is the reflection of light wave due to the screening effect of metal electrons to the incoming light. On the other hand, if $\omega > \omega_p$ the light wave gets transmitted, since the electrons in the metal are too slow and cannot respond fast enough to screen the field. For most metals, the specific value of $\omega_p$ lies in the ultraviolet region. This is the reason for their shininess and glittering nature in the visible spectrum. This treatment of a free electron gas gives quite accurate results for the optical properties of metals in the infrared region. The optical properties are determined mainly by the fact that the conduction electrons can move freely within the bulk of materials and the interband excitations can take place if the energy of the photons exceeds the band gap energy of the respective metal. For higher energy photons the Drude model becomes inaccurate due to promotion of electrons from lower lying bands to the conduction band.

## 2.5 Theoretical background:

### 2.5.1 Classical versus Quantum approach:

Nanoparticles are composed of several thousands to millions of atoms. The NPs can be assumed as the classical limits of electrodynamics, despite of their very small size compared to the classical objects. In contrast, surface plasmons are bosonic quasiparticles with true quantum nature established by tunnelling experiments.[17] Hence, it is theoretically rational to deal the plasmonic structures by classical electrodynamic approach as well as quantum mechanical treatment. The cumulative effects of many photons absorbed or emitted are considered as continuous macroscopically observable response. In this regard the classical description has been found appropriate to explain the optical properties of NPs in terms of Maxwell's equation. A rough estimation of the classical treatment has been justified for a high number of involved photons with their momentum small compared to the material system simultaneously.[18] By employing the *fluctuation dissipation theorem*, the dielectric response can be related to the dyadic Green tensor of Maxwell's theory to describe the linear response of metal NPs. Thus the quantum mechanical properties can be explained via dielectric functions such as ε and μ (frequency dependent dielectric function and magnetic permeability) which are obtained by experiments.

However the concept of dielectric function has been found insignificant for NPs with too small dimension (less than 5 nm). Although the optical properties of small metal clusters can be understood in terms of collective oscillations of valence electrons described by Drude model, a superior description has been obtained by adapting electronic structure methods. For smallest clusters the electronic structure theory interprets the optical properties in terms of discrete molecular like transition. In this account the time dependent density functional theory (TDDFT) has been found effective in dealing with optical properties of smaller as well as larger clusters ($Ag_{20}$ to $Ag_{120}$).[19] Besides dealing with single NP, the quantum nature of nanoparticle aggregates has been well described by TDDFT studies for dimmers of small clusters.[20-22] Recently an interest is growing in understanding the nature of nano aggregates as they provide a unique way of tuning the optical response by varying the distance between the NPs.[19-26] Due to excitation of plasmons an enhanced localized electric field can be found in the gap between the nanoparticles (the so-called hotspots). With decrease of the gap between the particles, the coupling increases, resulting to the very high electric fields. A very high electric field is found for separation below 5 nm where nonlocal dielectric effects are expected to be important.[27,28] It has been found even more apparent when the gap is reduced even further so that the particles are nearly touching.[19-26] In this regime electron tunnelling between the NPs takes place and modifies the optical response.[23] The clarification beyond phenomena has been well supported by quantum mechanical description while classical description has been found insignificant.

Hence in the present investigation, both the classical and quantum mechanical approach have been carried out to explore the optical nature of NPs. For larger NPs (~50 to 200 nm) the classical electrodynamic approach is adapted while for small NPs (~ 1 to 2 nm) quantum mechanical approach is executed.

### 2.5.2 Classical electrodynamics approach:

#### 2.5.2.1 Maxwell equations in matter

Electrodynamics correctly describes the time and spatial evolution of electromagnetic fields in the presence of charges, currents and any type of matter. The theory of electrodynamics developed by Maxwell in the 19$^{th}$ century, successfully described the interaction of magnetic and

electric fields and their propagation in the free space. When the local electric polarization of matter is designated with $\vec{P}$ and the local magnetization with $\vec{M}$, then two new fields $\vec{D}$ and $\vec{H}$ arise. These fields are defined as follow:

$$\vec{D} = \varepsilon_0 \vec{E} + \vec{P} \text{ and } \vec{H} = \mu_0^{-1} \vec{B} - \vec{M} \tag{2.3}$$

The constants $\mu_0$ and $\varepsilon_0$ are the permeability and permittivity of free space, respectively. The sources of these new fields $\vec{D}$ and $\vec{H}$ are the free charge density $\rho F$ and the current density $jF$, respectively. The forms of Maxwell equations are as:

$$\nabla \bullet \vec{D} = \rho F \tag{2.4}$$

$$\nabla \bullet \vec{B} = 0 \tag{2.5}$$

$$\nabla \times \vec{H} = j F + \frac{\partial}{\partial t} \vec{D} \tag{2.6}$$

$$\nabla \times \vec{E} = -\frac{\partial}{\partial t} \vec{B} \tag{2.7}$$

These equations have limitations. The constitutive forms of the equations are required to solve real problems like response of the materials. These forms are:

$$J_F = \sigma E, \quad B = \mu \mu_0 H, \quad P = \varepsilon_0 \chi E \tag{2.8}$$

The coefficients are conductivity, permeability and susceptibility respectively. These coefficients only depend on the medium under consideration and independent of the position and direction of the considered field. However these are frequency dependent. The time dependence forms of the fields are harmonic in nature.

$$E(\vec{r}, t) = E_\omega(\vec{r}) e^{-i\omega t} \tag{2.9}$$

The super position of such fields generates more complicated time dependent fields (Fourier synthesis). Introduction of all these equations into the Maxwells equation and simplifying the media without free charges to:

$$\nabla \bullet \left(\varepsilon \vec{E}\right) = 0 \tag{2.10}$$

$$\nabla \bullet \vec{B} = 0 \tag{2.11}$$

$$\nabla \times \vec{H} = -i\,\omega\varepsilon\, E \tag{2.12}$$

$$\nabla \times \vec{E} = +i\,\omega\mu\, \vec{H} \tag{2.13}$$

Here $\varepsilon$ is the complex dielectric function described by $\varepsilon = \varepsilon_0(1+\chi) + i\,\sigma\omega$. This set of equations together with the boundary conditions and conservation of energy and charge are sufficient to solve the time and spatial evolution of electromagnetic fields in the presence of matter.

### 2.5.3 Electrodynamic theories for particle plasmon:

A detailed understanding of plasmon resonance in NPs is described by classical electrodynamics. This approach has been developed based on material parameter like complex dielectric function $\varepsilon$.

#### 2.5.3.1 Quasi-static approximation — Rayleigh Theory:

Here a simplified quasi-static model proposed by Lord Rayleigh has been depicted for evaluation of particle plasmon. The self-induction effects i.e. retardation of electromagnetic fields are neglected. The electromagnetic phase is assumed constant throughout the region of interest since the region is considered much smaller than the wavelength of light. The simple electro-statics can be used to calculate the response of a metal sphere to an electric field as depicted in the following figure.

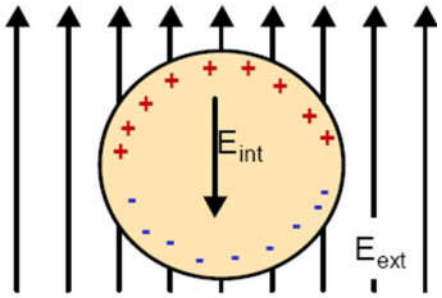


**Figure 2.4** Quasi-static model for particle plasmons.

It has been found reasonably simple for small metal particles with diameter below 40 nm where the microscopic dielectic function may be connected with microscopic polazability α. Thus the elastic scattering of light can be described in terms of Rayleigh scattering. Expressing the dipole moment $P$ through the local microscopic field and relating it with the dielectric function $\varepsilon$ (through $D = \varepsilon E = E + 4\pi P$) leads to the *Clausius-Mossotti relation* for spherical particles.[29]

$$\alpha = \frac{3V}{4\pi}\frac{\varepsilon_r - 1}{\varepsilon_r + 2} \tag{2.14}$$

Where $V$ is the volume and is the effective dielectric function. The expressions for the scattering and absorption cross section will be as:

$$C_{sca} = \frac{8\pi}{3}k^4|\alpha|^2, \qquad C_{abs} = 4\pi k\Im\mathrm{m}\{\alpha\}, \qquad C_{ext} = C_{sca} + C_{abs} \tag{2.15}$$

**2.5.3.2 Mie Theory:**

The response of spherical NPs to an external electromagnetic field can be calculated by solving Maxwell's equations. An analytical solution exists for uncharged spherical particles in a homogeneous medium. The exact analytical electrodynamical treatment is known as the Mie theory named after the developer Gustav Mie (1908).[30] Here a brief summary of main results derived by Bohren and Huffman (1982) has been stated.[31] The spherical symmetry suggests the use of a multipole extension of the fields, numbered by $n$. In Rayleigh type plasmon resonance

the dipole mode *n* is assumed 1. In the Mie theory, the scattering and extinction efficiencies are calculated by:

$$Q_{sca}^{(n)} = \frac{2}{x^2}(2n+1)\left(|a_n|^2 + |b_n|^2\right) \tag{2.16}$$

$$Q_{ext}^{(n)} = \frac{2}{x^2}(2n+1)\mathrm{Re}(a_n + b_n) \tag{2.17}$$

Here $x = kr = \hbar\omega r N_{medium}/(\hbar c)$, $k$ is wave vector, $r$ is particle radius, $N$ is refractive index, and $a_n$, $b_n$ are the Mie coefficients, which are calculated as:

$$a_n = \frac{m\psi_n(mx)\psi_n'(x) - \psi_n(x)\psi_n'(mx)}{m\psi_n(mx)\xi_n'(x) - \xi_n(x)\psi_n'(mx)} \tag{2.18}$$

$$b_n = \frac{\psi_n(mx)\psi_n'(x) - m\psi_n(x)\psi_n'(mx)}{\psi_n(mx)\xi_n'(x) - m\xi_n(x)\psi_n'(mx)} \tag{2.19}$$

Here $m = \sqrt{\varepsilon_r} = N_{particle}/N_{medium}$ and the Riccati-Bessel functions are $\psi_n$ and $\xi_n$.[31] These equations are applied in the calculation of scattering cross sections.

**2.5.3.3 Mie-Gans solution:**

An additional analytical solution for elliptical, spheroidal particles has been reported as Mie-Gans solution.[32, 33] This is the simple extension of the electrostatic theory for light scattering by spherical particles. Ellipsoidal particles are characterized by the three semi axes $a \geq b \geq c$. For spheroids two of these axes have identical length. The cigar shaped spheroids $(a > b = c)$ are called *prolate*, pancaked shaped $(a = b > c)$ are *oblate*. (Figure 2.5)

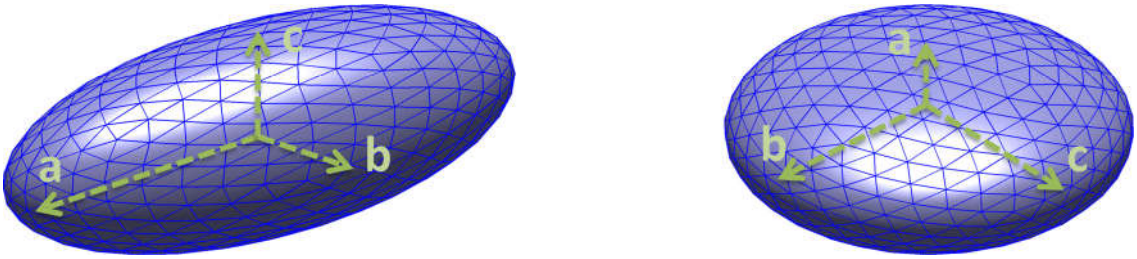


**Figure 2.5** Prolate (left, $a>b=c$) and oblate (right, $a<b=c$) ellipsoids.

The polarizability $\alpha_i$ of such a spheroidal particle along the axis $i$ is given by:[31]

$$\alpha_i = \frac{V\varepsilon_0}{L_i}\frac{1-\varepsilon_r}{(1/L_i - 1)+\varepsilon_r} \tag{2.20}$$

Here $L_i$ is the geometrical factor related to the shape of the particle. The sum rule $L_a + L_b + L_c = 1$ holds for $L_i$. Thus for a sphere $L_i$ = 1/3for all $i$. For an arbitrary ratio of the particle's semiaxis $a$, $b$ and $c$ the factor $L_i$ can be calculated as:[32]

$$L_i = \int_0^\infty \frac{abc\,ds}{2\left(s+a^2\right)^{3/2}\left(s+b^2\right)^{1/2}\left(s+c^2\right)^{1/2}} \tag{2.21}$$

## 2.6 Computational Modelling for larger NPs:

### 2.6.1 Numerical methods:

Numerical methods to solve Maxwell's equations became powerful tools to model NPs and plasmonic devices of arbitrary composition and shape. In the past few years, several numerical methods have been developed to determine the optical properties of small particles, such as the discrete dipole approximation (DDA), T-matrix and spectral representation methods (SR).[34] The DDA is a computational simulation suitable for studying scattering and absorption of electromagnetic radiation by particle with sizes of the order or less of the wavelength of the incident light. DDA has been applied to a broad range of problems, including interstellar and interplanetary dust grains, ice crystals in the atmosphere, human blood cells, surface features of

semiconductors, metal nanoparticles and their aggregates, and more. The DDA was first introduced by Purcell and Pennypacker[35] and has been subjected to several improvements, in particular those made by Draine and collaborators. [36] Here the main characteristics of DDA and its numerical implementation: the DDSCAT code has been discussed briefly.[34-36,37,38]

### 2.6.2 Discrete dipole approximation (DDA:

The main idea behind DDA is to approximate a scatterer by a large enough array of polarisable point dipoles. Once the location and polarizability of each dipole are specified, the calculation of the scattering and absorption efficiencies by the dipole array can be performed. The numerical problem is formulated as a set of $N$ linear (complex) non-homogeneous equations which for 3 dimensions takes the shape of a $3N \times 3N$ symmetrical matrix. The dielectric constant of the metal is introduced in the calculation by means of the polarizabilities. Usually 3D DDA calculations require less computational effort than finite differencing methods. This feature has made the DDA approach a powerful tool to model the optical properties of particles of different shapes and with dimensions of the order of a few hundred nanometres including studies of triangular prisms,[39] cubes,[40] truncated tetrahedral,[41] shell shaped particles,[42] disks[43] and rods,[44] among others.[45]

Let, an array of $N$ polarisable point dipoles located at $\{\mathbf{r}_i\}, i = 1,2,\ldots,N$, each one characterized by a polarizability $\alpha_i$. The system is excited by a monochromatic incident plane wave $\mathbf{E}_{\mathbf{inc}}(\mathbf{r},t) = \mathbf{E}_0 \mathbf{e}^{i\mathbf{k}\cdot\mathbf{r}-i\omega t}$, where $\mathbf{r}$ is the position vector, $t$ is time, $\omega$ is the angular frequency, $k = \omega/c = 2\pi/\lambda$ is the wave vector, $c$ is the speed of light, and $\lambda$ is the wavelength of the incident light. Each dipole of the system is subjected to an electric field that can be split in two contributions: (i) the incident radiation field, and (ii) the field radiated by all of the other induced dipoles. The sum of both fields is so-called local field at each dipole and is given by:

$$\mathbf{E}_{i,\mathbf{loc}} = \mathbf{E}_{i,\mathbf{inc}} + \mathbf{E}_{i,\mathbf{dip}} = \mathbf{E}_0 \mathbf{e}^{i\mathbf{k}\cdot\mathbf{r}_i} - \sum_{i \neq j} \mathbf{A}_{ij} \bullet \mathbf{P}_j \qquad (2.22)$$

Where, $\mathbf{P}_i$ is the dipole moment of the $i$th element, and $\mathbf{A}_{ij}$ with $i \neq j$ is an interaction matrix with 3×3 matrixes as elements, such that

$$\mathbf{A}_{ij} \bullet \mathbf{P}_i = \frac{\mathbf{e}^{ikr_{ij}}}{r_{ij}^3}\left\{k^2 \mathbf{r}_{ij} \times \left(\mathbf{r}_{ij} \times \mathbf{P}_j\right)\right\} + \frac{(1 - ikr_{ij})}{r_{ij}^2}\left[r_{ij}^2 \mathbf{P}_j - 3\mathbf{r}_{ij}\left(\mathbf{r}_{ij} \bullet \mathbf{P}_j\right)\right] \tag{2.23}$$

Here $r_{ij} = \left|\mathbf{r}_{ij} - \mathbf{r}_{ij}\right|$, and $\mathbf{r}_{ij} = \mathbf{r}_i - \mathbf{r}_j$, and cgs units are used. The 3*N*-coupled complex linear equations are given by the relation

$$\mathbf{P}_i = \alpha_i \mathbf{E}_{i,\mathbf{loc}} \tag{2.24}$$

Solving the above equation for dipole moment $\mathbf{P}_i$, one can sestimate the extinction and absorption cross sections for a target, $C_{\text{ext}}$ and $C_{\text{abs}}$ in terms of the dipole moments as

$$C_{\text{ext}} = \frac{4\pi k}{\left|\mathbf{E}_0\right|^2}\sum_{i=1}^{N}\left(\mathbf{E}_{i,\mathbf{inc}}^{*} \bullet \mathbf{P}_i\right) \tag{2.25}$$

$$C_{\text{abs}} = \frac{4\pi k}{\left|\mathbf{E_0}\right|^2}\sum_{i=1}^{N}\left\{\text{Im}\left[\mathbf{P}_i \bullet \left(\alpha_i^{-1}\right) * \mathbf{P}_i^{*}\right] - \frac{2}{3}k^3\left|\mathbf{P}_i\right|^2\right\} \tag{2.26}$$

Here * means complex conjugate. The scattering cross section is obtained by using the following relation (2.15):

$$C_{\text{ext}} = C_{\text{sca}} + C_{\text{abs}}$$

Hence, the coefficients of extinction ($Q_{\text{ext}}$), absorption ($Q_{\text{abs}}$) and scattering ($Q_{\text{sca}}$) are defined as follows:

$$Q_{\text{ext}} = \frac{C_{\text{ext}}}{A},\ Q_{\text{abs}} = \frac{C_{\text{abs}}}{A},\ Q_{\text{sca}} = \frac{C_{\text{sca}}}{A} \tag{2.27}$$

Where, $A = \pi a_{\text{eff}}^2$ and $a_{\text{eff}}^2$ is the effective radius of the shape with volume $4\pi\, a_{\text{eff}}^3/3$. The optical coefficients calculated using DDSCAT code are represented in the following Figure. 2.6

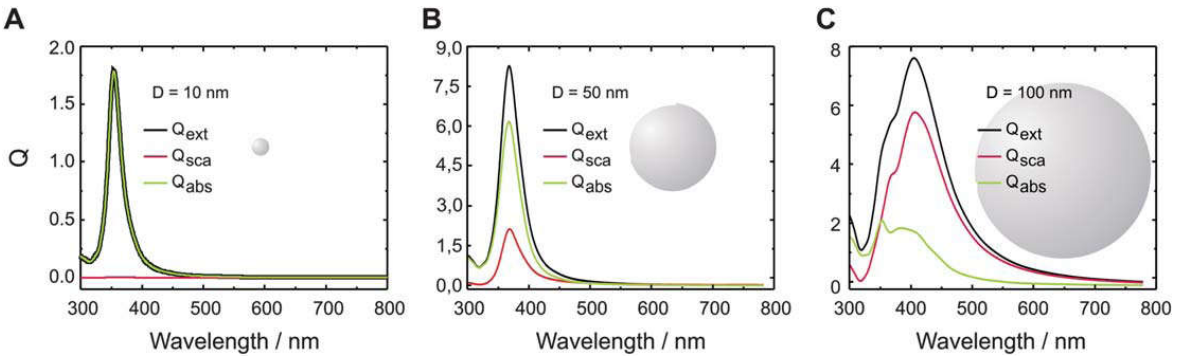


**Figure 2.6** Extinction, absorption and scattering efficiencies ($Q$) of spherical silver NPs (in vacuum) with increasing diameter ($D$).[46]

## 2.7 Microscopic origin of plasmon

With decrease of NP size the quantum effects predominate, which results manipulation in the optical property of NPs. This quantum nature enables small clusters to be treated with high level electronic structure. [47-59] In this context the electronic structure theory has been found in well agreement with the experimental results. This interprets the detail understanding of the fine structure in the absorption spectra. Thus the interplay between the accurate theoretical models and experimental results lead to an apparent description of electronic configurations of different geometries such as ground and excited state geometries. The fist-principle simulations have been found successful to describe the significant consequence of quantum effect on photo absorption spectra. [58, 60-62] The excellent agreement between the first-principle results and the experimental results describes the photo absorption spectra of NPs in terms of distinct molecular transition. Consequently, for larger clusters, the comprehensive analysis of the excitation using electronic structure theory becomes cumbersome due to the participation of large number of molecular transitions to construct the absorption band. For small clusters also the concept of surface plasmon cannot be interpreted with this viewpoint.[50] Therefore, it has been very crucial to come across a rational concept for concise interpretation of surface plasmon. Recently it has been explored that the electronic excitation can be interpreted as density oscillations even for very small clusters in support of time-dependent density functional theory (TDDFT) studies.[63,64] The density change due to the lowest excitation in $Na_2$ illustrated in the following Figure 2.7, clearly shows a density increase at one end of the molecule and a decrease at the other. Thus, the

excitations in small metal clusters in terms of transitions between distinct molecular states can be manifested by the collective electronic excitations arising from the oscillations of the valence electrons. Similar to the Na clusters, the absorption spectra for small Ag clusters has interpreted in terms of collective excitation of the valence electrons.[65-66] It has been possible to follow the evolution of cluster spectra from $Ag_{20}$ to $Ag_{120}$ by the TDDFT study.[19] The blue shift in the main absorption band of charged gold octahedral clusters with 6-146 atoms also has been explored with decreasing cluster size, through a TDDFT study.[67]

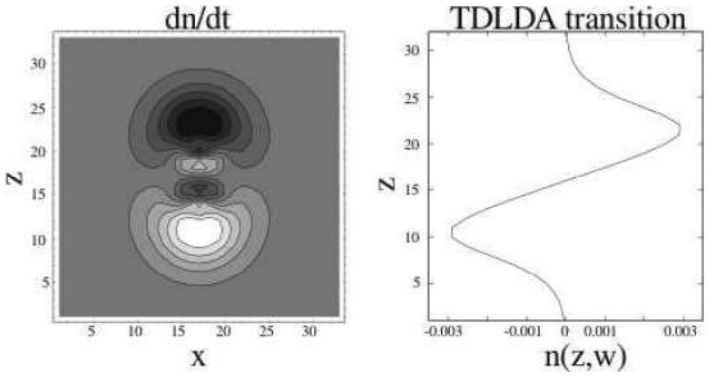


**Figure 2.7** Change in valence electron density using quantum fluid dynamics, where dark shading indicates a density decrease for the lowest excitation in $Na_2$. (left) Integrated electron density along the bond axis using TDDFT for the lowest excitation in $Na_2$. (right)[68]

### 2.7.1 Computatonal modelling for smaller NPs:

Several theoretical methods have been reported for modelling optical properties of NPs. First-principles modelling have been found convenient to provide accurate descriptions of the electronic structure and optical properties of Ag nanoclusters of different sizes.[50,69-76] TDDFT has also been applied to interpret optical properties for small and medium $Ag_n$ ($n$ = 2 22) clusters.[77-80] The *ab initio* techniques are well known for modelling the absorbance spectra for neutral $Ag_n$ clusters ($n$ = 2 8) and cationic $Ag_n^+$ clusters ($n$ = 2 4) using the framework of linear response equation-of-motion coupled cluster (EOM-CC) method.[81,82] A comparison between TDDFT and many-body method based on solving the Bethe-Salpeter equation (BSE) has been drawn for calculating the optical excitation of small $Ag_n$ ($n$ = 1 8) clusters.[80] Consequently TDDFT was found to be in good agreement with experiments, while poor

agreement was found for the BSE method, especially for the larger clusters. Recently, the long-range corrected TDDFT studies of absorption properties of $Ag_n$ ($n$ = 4  20) clusters showed improved agreement with experiments and EOM-CCSD results compared with traditional DFT functional.[83] In contrast to Na and Ag clusters, there have been several theoretical studies of the optical properties of small and medium sized Au clusters.[71,75, 84-90] The UV depletion spectra of $Au_n^-$. Xe ($n$ = 7  11) have been determined experimentally and compared with TDDFT simulations.[91] TDDFT predicted the optically allowed transitions for the most stable isomer of the corresponding Au clusters anions that were found to be consistent with the experimental observation. Overall, very good agreement between theory and experiments has been found, enabling a detailed understanding of the optical properties of the nano clusters to be achieved.

**2.7.1.1 Time-dependent density-functional theory:**

The Density Functional Theory (DFT) formalism cannot be used to extract information on excited states. Instead of the presence of the Hohenberg-Kohn theorem, DFT does not provide a practical way to write the excitation energies as a functional of the ground state density. The excited states can be successfully studied by an analogue to DFT, namely the time-dependent density-functional theory (TDDFT). The static non-relativistic many-electron Schrödinger equation describes the system of $N$ particles as

$$\hat{H}(\{r_i\})\Psi(\{r_i\}) = E\Psi(\{r_i\}). \tag{2.28}$$

Here $E$ denotes the total energy of the system and the Hamiltonian consists of terms related to the kinetic, interactions of electrons with themselves and external potential as

$$\hat{H}(\{r_i\}) = -\frac{1}{2}\sum_{i=1}^{N}\nabla_i^2 + \sum_{i<j}^{N}U(r_i, r_j) + \sum_{i=1}^{N}v_{\text{ext}}(r_i) \tag{2.29}$$

The total particle number $N$ is obtained by an integration of the amplitude of $\Psi(\{r_i\})$, over the whole space. Now the time-dependent, non-relativistic Schrödinger equation is as follow:

$$i\frac{\partial \Psi(\{r_i\},t)}{\partial t} = \hat{H}(\{r_i\}t)\Psi(\{r_i\},t) \tag{2.30}$$

Where, the initial wave function $\Psi_0$ is given. In 1984, Runge and Gross [92] derived the analogue of the Hohenberg-Kohn theorem for time dependent systems by establishing a one-to-one mapping between time-dependent densities $n(r,t)$ and time-dependent potentials $v_{\text{ext}}(r,t)$ for a given initial state.

From this time-dependent Schrödinger equation all the properties can be obtained of a system if electron density is known. From the time-dependent Kohn-Sham scheme the equation turns to

$$i\frac{\partial \psi_j(r,t)}{\partial t} = \left(-\frac{\nabla^2}{2} + v_{KS}[n](r,t)\right)\psi_j(r,t), \tag{2.31}$$

Here $\psi_j(r,t)$ is the Kohn-Sham orbital and $v_{KS}[n](r,t)$ is the Kohn-Sham potential, which is described as follow,

$$v_{KS}[n](r,t) = v_{\text{ext}}[n](r,t) + v_{\text{H}}[n](r,t) + v_{\text{XC}}[n](r,t) \tag{2.32}$$

There are two parallel alternatives for calculating the optical spectra within TDDFT. They are the linear response formalism and direct propagation in time. In the present dissertation the computational executions connected to TDDFT calculations are based on the linear response formalism, which has been stated briefly in the following section.

#### 2.7.1.2 Linear-response formalism:

In order to get the linear excitation spectrum, the linear-response theory is used to evaluate the susceptibility $\chi$. The first complete formulation of the response theory used today was done in 1985.[93] The starting point for a linear-response calculation is the first-order correction to the ground-state density that must produce the same density change in both the interacting and the Kohn-Sham system,

$$\delta n(r,t) = \int dt' \int d^3 r' \chi(r,r',t-t')\delta v_{\text{ext}}(r',t')$$

$$= \int dt' \int d^3 r' \chi_{KS}(r)(r,r',t-t')\delta v_{KS}(r',t') \tag{2.33}$$

Where, $\chi$ and $\chi_{KS}$ are the linear density-response functions of the interacting system and the Kohn-Sham system, respectively. From the relation (2.32) the relation between the potentials is

$$\delta v_{KS}(r,\omega) = \delta v_{\text{ext}}(r,\omega) + \int d^3 r' \frac{\delta n(r,\omega)}{|r-r'|} + \int d^3 r' f_{\text{xc}}(r,r',\omega)\delta n(r',\omega) \tag{2.34}$$

Introducing the Fourier transform of the time-dependent kernel

$$f_{xc}(r,r',t-t') = \frac{\delta v_{\text{ext}}(r,t)}{\delta n(r',t')} \tag{2.35}$$

The Fourier transformation of Eq. (2.33) to the frequency space and use of linear perturbation theory, forms the Dyson-like equation for the $\chi$ of the interacting system.

$$\chi(r,r',\omega) = \chi_{KS}(r,r',\omega) + \int d^3 r'' \int d^3 r''' \chi_{KS}(r,r'',\omega) \times \left( \frac{1}{|r''-r'''|} + f_{\text{xc}}(r'',r''',\omega) \right) \chi(r''',r',\omega)$$

(2.36)

The full solution for Eq. (2.36) is still numerically difficult. Following the notation by Casida[94] and Petersilka,[95] the problem can be turned into solving the eigenvalue problem after a considerable amount of algebra.

$$\boldsymbol{Q}\boldsymbol{F}_I = \Omega_I^2 \boldsymbol{F}_I \tag{2.37}$$

Above $\Omega_I$ denotes the $I$ th excitation energy and the eigenvectors $\boldsymbol{F}_I$ can be used to obtain the oscillator strengths. The matrix elements of $Q$ are given by

$$\boldsymbol{Q}_{ij,kl} = \delta_{i,k}\delta_{j,l}\omega_{kl}^2 + 2\sqrt{\omega_{ij}}\boldsymbol{K}_{ij,kl}\sqrt{\omega_{kl}} \tag{2.38}$$

Where, $i$ and $k$ run over the unoccupied states and $j$ and $l$ over the occupied states. $\omega_{ij} = \varepsilon_i - \varepsilon_j$ are the differences between the energy eigenvalues of the single-particle states. $K$ is a coupling matrix with elements

$$K_{\substack{i,k \\ j,l}}(\omega) = \iint \psi_i^*(r)\psi_j^*(r)\left(\frac{1}{|r-r'|} + f_{\mathrm{xc}}(r,r',\omega)\right)\psi_k(r')\psi_l(r')d^3rd^3r'. \tag{2.39}$$

Above, adiabaticity has been assumed. Consequently, the matrix $Q$ is independent of the excitation energy. For exchange-correlation functionals with memory this does not hold and the non-linear eigenvalue problem, $\boldsymbol{Q}(\Omega_I)\boldsymbol{F} = \Omega_I^2 \boldsymbol{F}_I$, has to be solved self-consistently.

Recently, the development of improved linear-response kernels derived from many-body perturbation theory has been successful. [96,97] Two different classed of such approaches are being developed. The first one is based on approximated exchange-correlation functional or on the Sham-Schlüter equation, which impose the many-body density equal the DFT one. The second class assumes the Kohn-Sham and quasiparticle states to be the same, targeting to a kernel which can account for the electron-hole interaction and the excitonic effects provided by the Bethe-Salpeter equation. This development brings TDDFT a promising method to calculate the electronic spectra even for extended systems.[95] Recently, the linear response TDDFT method, typically the Casida method, has been included in all advanced computational chemistry packages that are based on DFT.